

## The trigger system of the Telescope Array detector

M. Sasaki<sup>1</sup>, T. Aoki<sup>1</sup>, Y. Arai<sup>2</sup>, M. Fukutomi<sup>3</sup>, K. Hashimoto<sup>4</sup>, K. Honda<sup>5</sup>, F. Ishikawa<sup>1</sup>, M. Jobashi<sup>1</sup>, N. Manago<sup>1</sup>, M. Masuda<sup>1</sup>, M. Sakai<sup>3</sup>, Y. Tanaka<sup>3</sup>, Y. Tsujikawa<sup>6</sup>, and the other Telescope Array collaborators

<sup>1</sup>Institute for Cosmic Ray Research, Univ. Tokyo, Kashiwa, Japan

<sup>2</sup>High Energy Accelerator Research Organization, Tsukuba, Japan

<sup>3</sup>Department of Electrical Engineering, Nagasaki Institute of Applied Science, Nagasaki, Japan

<sup>4</sup>Faculty of Education and Human Science, Yamanashi University, Kofu, Japan

<sup>5</sup>Faculty of Engineering, Yamanashi University, Kofu, Japan

<sup>6</sup>Faculty of Science, Konan University, Kobe, Japan

**Abstract.** This note describes the trigger system of the Telescope Array detector and its performance from the prototype tests.

### 1 Introduction

The TA detector has been designed to explore new physics processes occurring in the big bang early universe and enormously active terrestrial accelerators in the extra-galaxy. The general detector design is given elsewhere (Sasaki et al., 1997) (TA Design Report, 2000).

### 2 Design Requirements

The strength and duration of air-fluorescence light pulse from an air-shower event largely depends on the kinematics and atmospheric extinction. For example, Fig.1 shows the difference between simulated wave form digitized by 5MHz-sampling ADC for vertical and inclined air-showers. Monte Carlo studies have shown that integrating of the charge successive signal followed by digitization with a 5MHz-ADC satisfies the resolution requirements and has adequate dynamic range (Sasaki et al., 2001).

The overall signal to noise ratio (S/N) in view of a PMT is approximately given by:

$$\frac{S}{N} = N_e N_\gamma c \frac{1 + \cos \theta}{4\pi R_p^2} e^{-\tau/\lambda_R} \left( \frac{\epsilon A}{4B\Delta\Omega} \right)^{1/2} \left( \frac{\Delta t_s}{\Delta t_I^{1/2}} \right) \propto E \left( \frac{D^3}{d} \right)^{1/2},$$

explicitly showing the mismatch between the integration time  $\Delta t_I$  and the signal duration time  $\Delta t_S$  where  $A$  is the optical gathering area and  $\lambda_R$  is the Rayleigh scattering length,  $N_e$  is

Correspondence to: M. Sasaki (sasakim@icrr.u-tokyo.ac.jp)

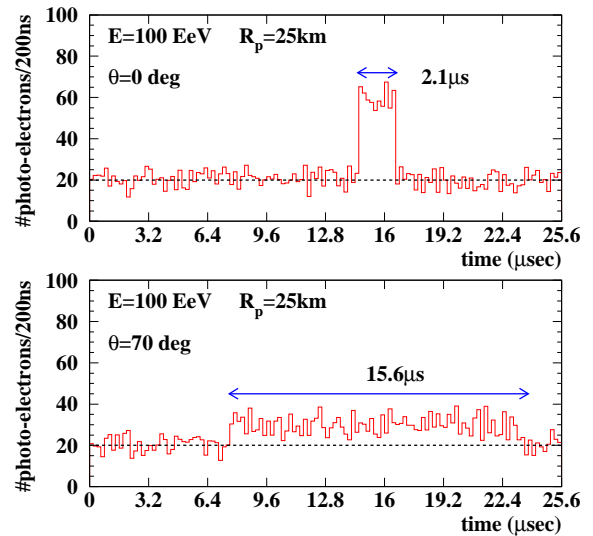


**Fig. 1.** Typical simulated PMT signals digitized by 5MHz-ADC for different event geometry of  $10^{20}$ eV proton induced air-showers. Vertical (top) and deeply-inclined (70 degree; bottom) cases are shown. Impact parameter and night sky background are commonly assumed to be 25 km and 20 photoelectrons/200ns/PMT respectively.

the number of electrons in the air-shower, and  $N_\gamma$  is the fluorescent yield. The measured S/N also depends on the primary energy of the air-shower and the optical factor where  $d$  and  $D$  are the diameters of the PMT and mirror aperture respectively.

For further optimization of S/N can be done by maximizing the factor of  $(\Delta t_s/\Delta t_I^{1/2})$ . A priori one does not know this  $\Delta t_s$  since it is event dependent. Events detected by the TA detector can generate pulses whose widths range from several tens ns to several tens  $\mu$  s. Hence, to take full advantage of time integration in minimizing noise, we have employed an on-flight signal recognition with optimizing vari-

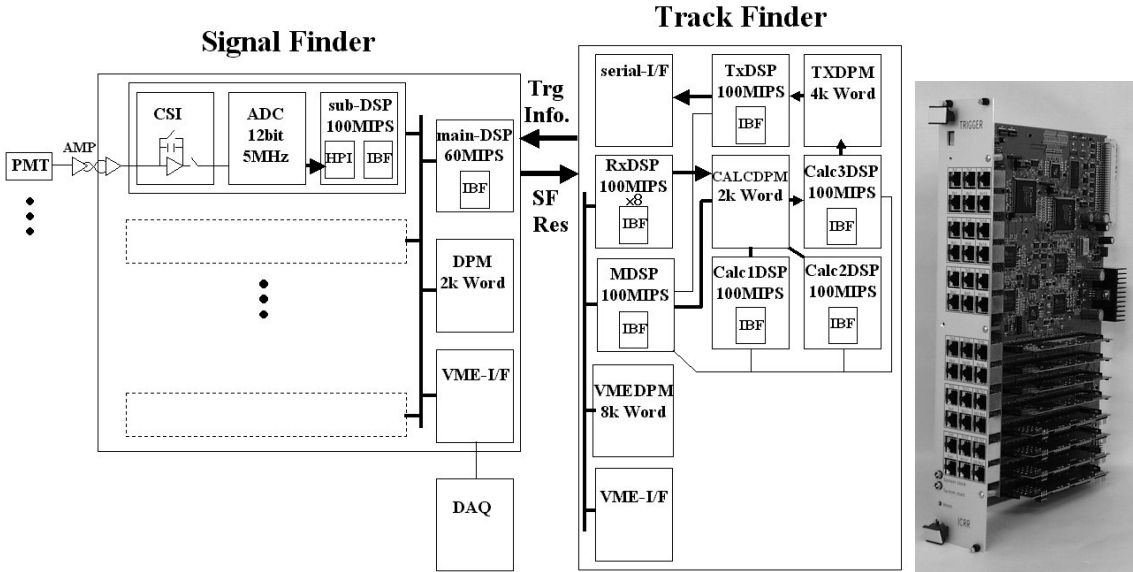


Fig. 2. Block diagram of Signal Finder and Track Finder (left) and photograph of a prototype module of Track Finder.

able time filter by ch-by-ch parallel digital signal processors (DSPs) in order to trigger on nearby as well as distant events with optimum efficiency without strong bias for or against specific time duration of signal wave form. Assuming the optimized efficiency for triggering, we convert electron size  $N_e$  to energy in order to obtain an estimate for energy triggering thresholds. We take (Gaisser and Hillas, 1977):

$$E = 1.6 \times 10^{-9} N_e ,$$

where  $E$  is the primary energy in EeV. Also assuming  $r = R_P$  and the TA optical design, a crude estimate of the energy threshold is given by:

$$E_{th}[\text{EeV}] = 10^{-4} \left( \frac{S}{N} \right) R_P^{3/2} e^{R_P/\lambda_R} ,$$

where  $R_P$  is in km. This simple estimate suggests that the sensitive TA detector optics and readout devices should allow us significantly lower energy threshold of  $10^{16}$  eV and larger detection aperture. It also provides richer physics objects like detection capabilities of statistically significant detection of the AGN neutrino and fairly precision test of change of elongation rate in the wider energy range.

The rate of air-shower events with the energy of  $10^{16}$  eV in the condition that the signal to noise ratio at least in one PMT should be more than one is estimated to be 0.2 Hz per camera with 256 PMTs equipped from Monte Carlo study. The night sky background photoelectrons are dominant component in these flows at the rate of 20~30 photoelectrons per ADC sampling time of 200ns in each PMT. We can safely assume that the trigger rate from a detector station should be less than 10 Hz even taking into account faked triggers due to background pick-ups.

### 3 System Design

The frontend trigger electronics consists of Signal Finder (SF) and Track Finder (TF) to recognize air-shower events in a most powerful test way as shown in Fig. 2.

The TA camera installed on a telescope consists of 256 PMTs. A pretrigger cluster is defined as a set of 4x4 adjacent PMTs. The wave form signals from 16 PMTs in a pre-trigger cluster are sent to a SF module implemented on 9U-VME board. All analog signal amplified by pre-amp circuits mounted near PMTs are successively sent to the SF modules and stored into host port interface (HPI) memories inside of individual digital signal processor (DSP) just after analog-to-digital conversion (ADC). SF provides recognized signal features for each PMT wave form and send the resultant information to TF synchronously every  $25.6\mu\text{s}$ . SF keeps all digitized wave form on the internal buffer memories until receiving Data Acquisition (DAQ) request from TF or overwriting of new data at the cycle of 3ms corresponding to the buffer memory depth. Also, every  $25.6\mu\text{s}$ , TF receives the SF information and send back the recent track-finding result indicating the wave form data address on SF-DSP internal memories to sweep out then into DAQ devices. The epoch-making is that every PMT-signal is processed by individual DSP on-flight software programs with real time method as well as track finding and data flow controls, which compose the triggering system.

### 4 Signal Finding

On one SF module, sixteen individual TI-C549 DSPs for signal finding and one module DSP are implemented. The TI C549 DSP for signal finding has a performance of 100 MIPS. The module DSP for data flow control has a performance of 60 MIPS. Even if using such a high-performance DSP, a so-

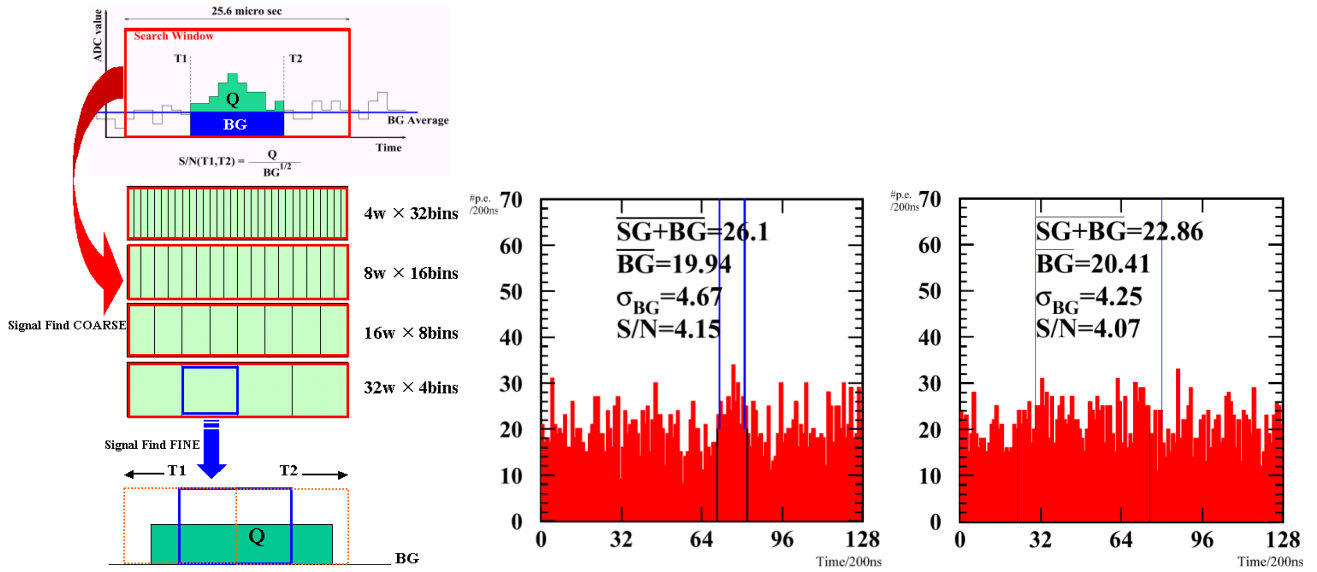


**Fig. 3.** Signal finding algorithm with coarse and fine search processes (left), demonstration of signal finding tests for short wave form (middle) and long one (right). The two upper lines show true starting and ending times of input signal. The two lower lines show found ones.

phisticated signal finding algorithm is mandatory. DSP runs signal finding algorithm (Fig.2 and 3) as follows:

1. Each SF-DSP defines the address region to search with the length of  $25.6\mu\text{s}$  corresponding to 128 words of ADC-data.
2. Maximize  $S/N(T1,T2)=Q/\sqrt{B}$  changing T1 and T2 independently where Q is a charge sum between T1 and T2 and B is background averaged from average of past data not triggered.
3. In order to search the optimum S/N efficiently, each SF DSP performs two stages of search process, coarse search and fine one.
4. In the coarse search, the search window of  $25.6\mu\text{s}$  corresponding to 128 ADC-data is subdivided into four combinations of bins like 4 words  $\times$  32 bins, 8 words  $\times$  16 bins, 16 words  $\times$  8 bins, and 32 words  $\times$  4 bins. The DSP program finds a certain bin of which estimated S/N is larger than any others.
5. After the coarse search, the program starts a finer adjusting algorithm. It finds further increase of S/N as changing the starting and ending edges, T1 and T2, bin by bin around these found by the coarse search. And finally DSP program finds out the maximum S/N in the search window of 128 words.
6. Signal finding DSP send the determined T1,T2 , and Q to the dual port memory (DPM) to communicate with the module DSP.
7. The module DSP gathers the signal finding results from DPM and packs them into one serial packet.

8. The module DSP sends the serial packet of determined signal finding results to the event trigger track finding module via fast serial connection with a buffered serial port on the RxDSP of the TF module. The serial connection has a transfer rate is 50 Mbps.
9. The wave form data of 128 words are kept on the internal buffer memory of individual DSP. The buffer depth corresponds to 3ms so that it can wait for the TF result as DAQ request in 3ms. If there is no DAQ request from TF within 3ms after the search, the memory area is overwritten by new ADC data.

We have developed and tested sixteen SF prototype-modules corresponding to 256 PMT input channels. It has been confirmed that the hardware works fine with the input circuit noise less than two photoelectrons, which is equivalent to less than half of fluctuation of night sky background  $\sqrt{30}=5.5$  photoelectrons, and good linearity with 16 bits of dynamic range. Also above DSP signal finding algorithm has been implemented onto SF-DSPs completely with dedicated assembler language. The software can perform the algorithm and data flow control well without any dead time. The SF algorithm and the demonstrations are shown in Fig. 3. As we tested, the algorithm recognize signals pulse timing and its charge fairly well for the real input signal wave in the case of S/N more than 2.5. According to a Monte Carlo study, the charge resolution by this algorithm is 40% for 10 photoelectrons ( $Q=10$ ) and 20% for 40 photoelectrons.

## 5 Track Finding

The TF module for event triggering essentially investigates the 3D-pattern in the (X, Y, T) space where X, Y stands for

the PMT center position on the optical focal plane of the detector station and T for the T1 or T2. A prototype of TF has been developed (Fig. 2) and now it is under test. The data flow on the module is described as follows:

1. One TF module has 8 RxDSPs which have two buffered serial ports responsible for inputs from two SF modules respectively. Each buffered serial port on RxDSP receives each set of T1, T2, and Q synchronously every  $25.6 \mu\text{s}$ .
2. The RxDSP quickly recognizes mutually connected in (X,Y,T) 3D-coordinates out of SF results in a pretrigger PMT cluster. And it calculates the total S/N for the cluster from chosen sets of T1, T2, and Q.
3. The RxDSP sends out the data of the resultant cluster-S/N and all 16 sets of signal finding results to 4-port memory (CALCDPM) via the module bus. The transfer timing is well scheduled not to interfere with each other on the module bus. Just after all RxDSPs finish transferring the cluster results, interrupt signals are sent to three DSPs (Calc1DSP, Calc2DSP, and Calc3DSP) for track finding calculation in order to inform them data-ready.
4. The Calc1DSP judges pretrigger with all 16 cluster-S/Ns. The total S/N with only signals in clusters mutually connected out of 16 clusters on one camera in the 3D-coordinates is calculated similarly to the previous S/N extracted from a pretrigger cluster. The total S/N for camera (camera-S/N) is used to finally determine the pretrigger. The pretrigger threshold must be decided from detailed Monte Carlo studies or real pilot observations.
5. Calc1DSP also determines the center of gravity (c.o.g.) of the 3D-pattern for pretriggered events.
6. Calc2DSP searches track of 3D-pattern of (X,Y,T) again (Fig. 4) from the c.o.g. using all signal finding informations including wider time region.
7. Calc3DSP calculates the total S/Ns from the selected patterns by Calc2DSP. After that, it finds the largest S/N from signal informations close to the optimum track and judge the final trigger decision. The result of the trigger judgement is sent to a dual port memory (TXDPM) followed by TxDSP.
8. TxDSP always watch the trigger judgement on TXDPM. Once it gets the trigger judgement, The TxDSP make a serial packet to inform corresponding SF modules the window identification to indicate memory address which stores the triggered wave form data. The TxDSP send the packet data onto serial interface port. Finally SF module receives the distributed window identification as a DAQ request.

We have confirmed the data flow in both the SF and TF prototypes are well controlled synchronously. From the detailed Monte Carlo studies, we have investigated the efficient

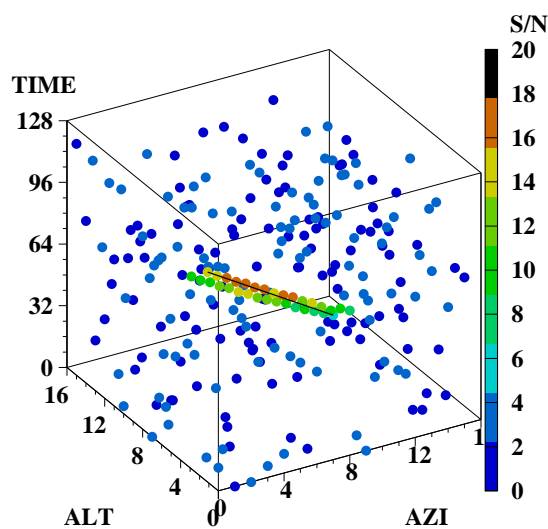


Fig. 4. Simulated results of signal finding for  $10^{18}$  eV air-shower and night sky background.

pretrigger condition. The camera-S/N is totally biased by approximately 4 due to maximizing S/N in the series of SF, cluster-S/N, and camera-S/N algorithm. For instance, calculated camera-S/N only from simulated night sky background has a distribution of which mean is 5.0. If we adopt  $S/N > 7$  as the pretrigger threshold cut, the background contamination can be reduced by factor 40. In the same condition, the pretriggered aperture for air-shower events with the primary energy of  $10^{17}$  eV is estimated to be  $9.5 \times 10^3 \text{ km}^2 \text{ sr}$ , which corresponds to the event rate of 0.05 Hz in a camera. At next step, track finding after pretrigger needs to reduce the background further more by factor 100 without strongly sacrificing the efficiency for the air-shower events. The sophisticated 3D-pattern track finding algorithm and the DSP program are now under developing.

## References

- Sasaki, M., et al, Proc. 25th ICRC, 5, 369 (Durban, 1997).  
 The Telescope Array Project: Design Report. July 2000.  
<http://www-ta.icrr.u-tokyo.ac.jp>  
 Sasaki, M., et al, Frontend Electronics of the Telescope Array Detector, Proc. 27th ICRC, HE1.7 (Hamburg, 2001).  
 Gaisser, T. and Hillas, A., Proc. 15th ICRC, 7, 353 (Plovdiv, 1977).